Self-Pulsation Dynamics in Narrow Stripe Semiconductor Lasers

Pascal Landais, *Member, IEEE*, Stephen A. Lynch, *Senior Member, IEEE*, James O'Gorman, Ingo Fischer, and Wolfgang Elsäßer, *Senior Member, IEEE*

***Abstract*—In this paper, we address the physical origin of self-pulsation in narrow stripe edge emitting semiconductor lasers. We present both experimental time-averaged polarization-resolved near-field measurements performed with a charged-coupled device camera and picosecond time resolved near-field measurements performed with a streak camera. These results demonstrate dynamic spatial-hole burning during pulse formation and evolution. We conclude from these experimental results that the dominant process which drives the self-pulsation in this type of laser diode is carrier induced effective refractive index change induced by the spatial-hole burning.**

***Index Terms*—Self-focusing, self-pulsation (SP), semiconductor lasers, spectral-hole burning, wave-guide.**

I. Introduction

SELF-PULSATION (SP) is the term commonly used to describe the pulsed emission obtained from certain laser diodes when operated under dc bias. The phenomenon has been known from the early days of semiconductor lasers [1]–[4], and has been exploited to beneficial effect in several optoelectronic based devices. The origin of SP in laser diodes varies according to the device structure. In laser diodes which have a saturable absorber adjacent to the gain section, such as CD or DVD edge-emitting lasers (EELs) [5], or vertical-cavity surface-emitting lasers (VCSELs) [6], the SP is explained using bifurcation theory and is understood to be undamped relaxation oscillations [7], [8]. In the case of single mode distributed feedback (DFB) lasers, an explanation based on a dispersive Q-switching has been published [9], [10]. An alternative explanation relies on presence of a negative effective differential gain [11]. In some multimode DFB lasers, the SP can be attributed to a periodic switching between two modes due to a mode competition [12], [13]. In multisection DFB lasers, the possibility of spatial instability was investigated [14]. Mode beating where SP frequencies up to 100 GHz corresponding to the frequency difference between two consecutive lasing modes selected by the subcavities has also been demonstrated [15]. Very recently evidence for passive mode-locking in DBR lasers has been published [16]. Other reports of SP in DBR lasers have attributed the origin of the SP to four-wave mixing [17], [18].

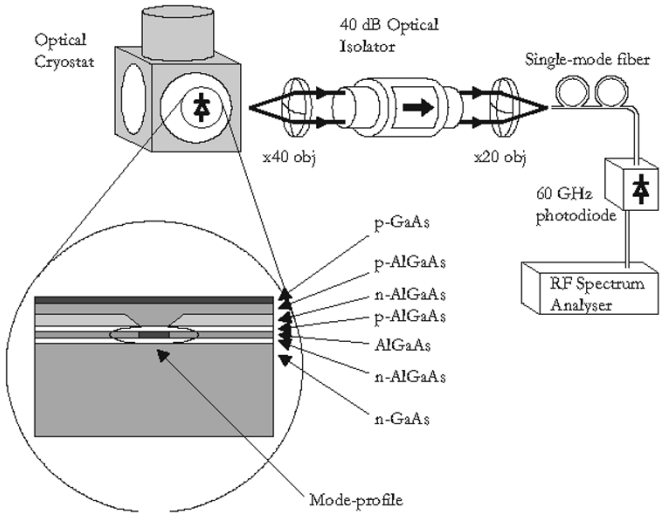

Fig. 1. Schematic of the experimental setup. Inset shows the structure of the narrow stripe laser.

SP lasers have multiple applications. In all-optical telecommunications systems, the SP laser can be used: 1) to retrieve the bit-rate of an incoming return-to-zero data signal [19]; 2) as chaotic carrier in secure systems [20], [21]; or 3) as RF carrier for hybrid RF-optical networks [22]. In optical storage systems, SP lasers are currently used in CD and DVD players. SP lasers are advantageous in these applications since their short coherence length makes them less sensitive to optical feedback and leads to a very low relative intensity noise [23].

In this paper, we present a detailed experimental investigation of the SP phenomenon in CD lasers, leading to a more complete understanding of the origin of SP in these devices. The conventional CD laser is a narrow stripe component as shown in Fig. 1. The laser diodes are designed so that the lateral electromagnetic field extends from an electrically pumped region of the stripe layer to unpumped regions on either side which act as saturable absorber sections. Lateral charge carrier transport effects in the nonuniformly pumped stripe layers would, therefore, play a strong role since it is well known that they affect the damping of relaxation oscillations in bulk active region lasers [24]–[27] and quantum-well structures [28]. In our

Manuscript received September 22, 2005; revised January 13, 2006. The work of S. A. Lynch was supported in part by Forbairt research scholarships.

P. Landais is with the School of Electronic Engineering, Dublin City University, Dublin 9, Ireland (e-mail: landaisp@eeng.dcu.ie).

S. A. Lynch is with the Semiconductor Physics Group, Cavendish Laboratory, University of Cambridge, Cambridge CB3 0HE, U.K. (e-mail: sal44@cam.ac.uk).

J. O'Gorman is with Eblana Photonics, Trinity College Enterprise Centre, Dublin 2, Ireland (e-mail: james@eblanaphotonics.com).

I. Fischer is with the Department of Applied Physics and Photonics, Vrije Universiteit Brussels, B-1050 Brussels, Belgium (e-mail: ifischer@tona.vub.ac.be).

W. Elsäßer is with the Institut für Angewandte Physik, Technische Universität Darmstadt, D-64289 Darmstadt, Germany (e-mail: elsaesser@physik.tu-darmstadt.de).

Digital Object Identifier 10.1109/JQE.2006.872309

previous work, however, it was shown that strongly temperature-dependent effects (such as charge carrier diffusion) do not play a key role in the pulse generation in the CD lasers [29], [30]. In order to develop further understanding of the SP mechanism in this type of laser structure, we have performed a series of measurements to observe the influence of spatial-hole burning on the effective refractive index of the waveguide. The paper is organized as follows. In Section II-A, the laser performances are described with an emphasis on the SP behavior as a function of temperature. In Section II-B and C, results concerning investigations of the near-field at the output facet are discussed both in terms of time averaged and real-time measurements. These observations have allowed us to develop a better understanding of the mechanism leading to the generation and evolution of pulses in narrow-stripe EELs. The genesis of the pulses is further discussed in Section III and finally conclusions are drawn in Section IV.

II. Experimental Investigations

A. General Experimental Considerations

We characterized four SHARP LT022MD laser diodes over a wide range of operating conditions and found the behavior of each device to be very similar. As far as possible we have tried to present the experimental trends from one representative device in order to preserve some element of consistency throughout the paper. The structure of these devices is illustrated in the inset of Fig. 1. The laser consists of a Fabry–Perot cavity with a bulk AlGaAs active region with emission wavelength at 800 nm. The gain section is pumped through a p-type electrical contact and has the following approximate dimensions: 250 μm long, 2 μm wide, and 0.2 μm thick. The two n-blocking layers confine the current to the central region of the active layer, resulting in two lateral unpumped regions at either side. The tails of the optical mode propagating along the laser cavity overlap with these electrically unpumped regions. During the cycle of pulse emission the interband optical absorption in these electrically unpumped regions becomes saturated. The resulting change in carrier density causes a related change in the complex refractive index, thereby changing the transverse guiding and losses as the pulse is emitted.

As illustrated in Fig. 1, the device is placed in a liquid nitrogen cooled optical cryostat which allowed temperature tuning in the range, $77\ \text{K} \leq T \leq 370\ \text{K}$. The emitted light is then collected by a 0.65-NA microscope objective and passes through a 36-dB optical isolator to avoid any feedback which could influence the SP behavior. At the isolator output the light is monitored by either an integrating sphere (not illustrated) or a 60-GHz bandwidth photodiode. The integrating sphere is used to record calibrated, time averaged power measurements.

Fig. 2 shows the typical light–current (L–I) behavior of this type of laser diode measured with an integrating sphere and for various heatsink temperature range. Between 150 and 370 K, the L–I behavior is linear above threshold. However below 150 K, the L–I curves develop significant nonlinearities which increase in amplitude with decreasing temperature. This observed behavior can be explained as a change in the modal gain, since the slope efficiency dL/dI between the threshold current and the nonlinearity is different from the slope efficiency above the nonlinearity. This change in the modal gain is due to perturbations in refractive index and gain resulting from spatial burning. This is confirmed by experimental measurements of the near-field at the output facet detailed in Section II-B (see explanation related to Fig. 7).

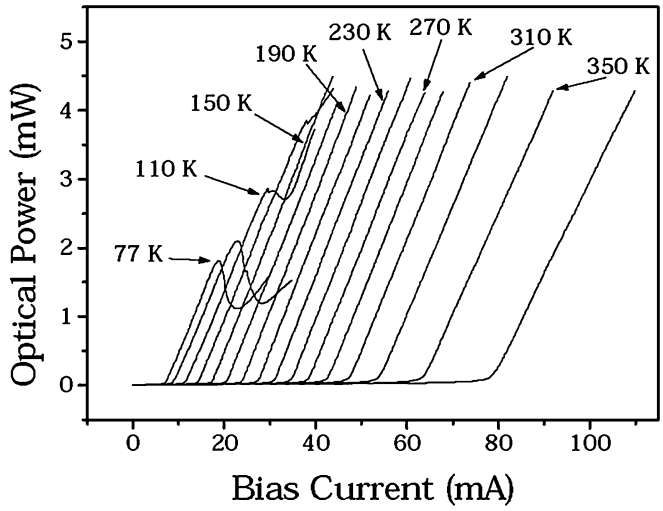

Fig. 2. Typical L–I curves for a SHARP LT022MD in the temperature range, $77\ \text{K} \leq T \leq 370\ \text{K}$. Note: Only every second curve is labeled on the graph. Below 110 K, no SP was observed.

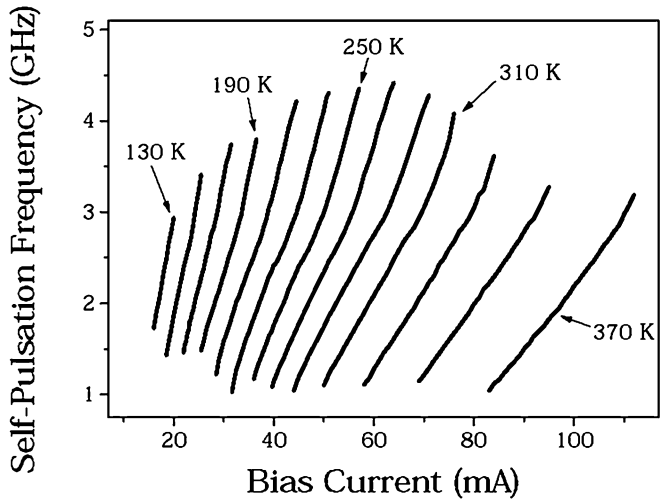

Fig. 3. SP frequency versus bias current measured at 20-K intervals, in the temperature range $110\ \text{K} \leq T \leq 370\ \text{K}$. Note: Only every third curve is labeled on the graph. Below 110 K, no SP was observed.

Next, we investigate the fundamental frequency of the SP as a function of bias current. The 60-GHz photodiode was used to transform the optical emission to an electrical signal which was observed with a 22-GHz bandwidth RF spectrum analyzer. Fig. 3 shows the SP frequency versus bias current over the same temperature range. Self-pulsation is extinguished at 130 K approximately. This suggests that there is a relationship between the temperature induced effects on the parameters of the laser and the generation of the SP. To gain further understanding we carried out polarization-resolved L–I characteristics at 370 and 77 K.

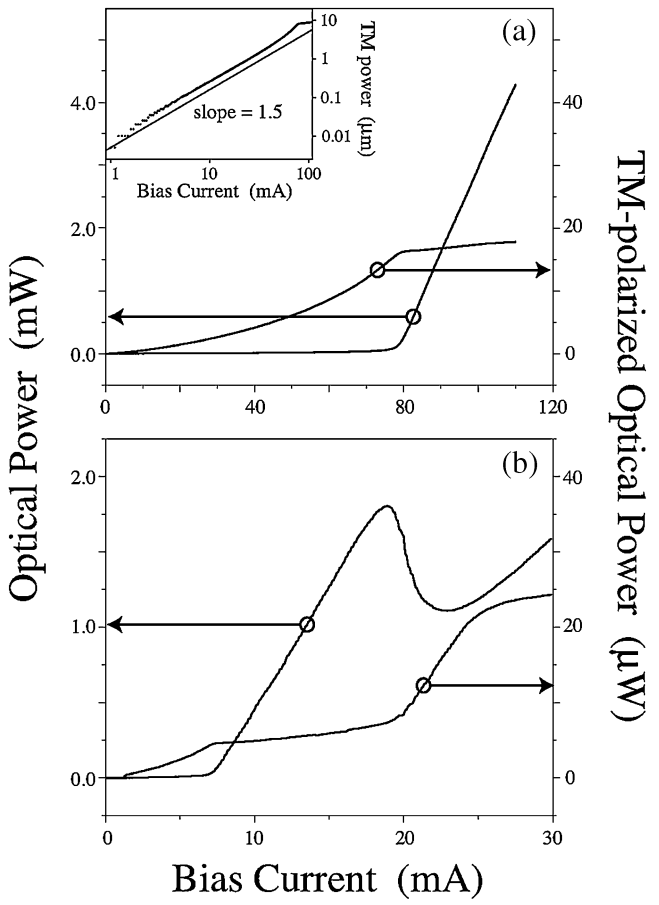

Fig. 4. L–I curves for a SHARP LT022MD laser diode (a) at a heatsink temperature of 370 K, on the left axis polarization unresolved and on the right axis, TM-polarization resolved. Inset: TM-polarization resolved L–I curve is expressed in log–log plot. The full line shows a 1.5 power law dependence. (b) Similar plots at a heatsink temperature of 77 K.

For a slab waveguide, only two types of guided transverse modes are supported, i.e., transverse electric (TE) and transverse magnetic (TM). For TE modes, the polarization of the guided light is aligned along the plane of the active layer and for TM modes the polarization is aligned along the growth direction. CD laser diodes are designed to emit predominantly in the TE mode, since it has a slightly larger confinement factor and facet reflectivity. One practical consequence of this fact is that it provides a way to probe the transverse carrier distribution, since a crossed polarizer can be used to effectively block the TE lasing mode. The remaining light will then be mainly due to spontaneous emission related to the carrier density through a quadratic dependence.

Fig. 4(a) and (b) shows the polarization-resolved L–I characteristics for heatsink temperatures of 370 and 77 K, respectively. Our lasers have their lasing emission in the TE mode. On the left axis of each graph, we have plotted the nonpolarization-resolved L–I curve and on the right axis the TM-polarized L–I curve recorded through a Glan–Thompson polarizer. In Fig. 4(a), the polarization unresolved L–I curve shows a threshold current at 80 mA approximately and a collected emission of about 4.5 mW at 110 mA. The TM-polarization-resolved L–I behaves according to a power law up to 80 mA. As shown in the inset, the

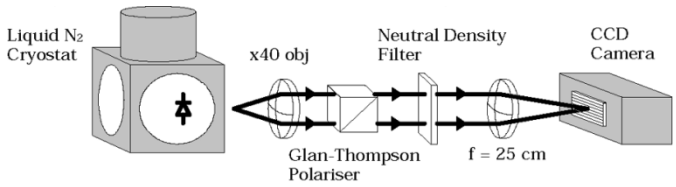

Fig. 5. Schematic of the experimental setup used to investigate the near-field.

exponent of this power law is equal to 1.5. Above the threshold current, the TM-polarized light collected does not continue to increase with current, but it does not saturate either. Under the same experimental light collection conditions, the TM-polarized optical power is less than 20 μW at 100 mA, compared to the nonpolarization-resolved optical power of 3 mW. In theory, the carrier density in a mono-section laser becomes clamped at threshold. In our experiment, the increase in the TM emission and consequently in the carrier density can be explained by gain suppression resulting from spatial, spectral-hole-burnings, and carrier heating. Above threshold, any further increase in current leads to stimulated emission. This type of behavior happens down to $\sim$150 K. Fig. 4(b) is recorded at $T = 77$ K. The TM-polarization-resolved curve appears to pin once at the threshold level and for a second time at higher level around the nonlinearities observed in the nonpolarization resolved L–I curve. We have performed a near-field observation of one of the output facets to get further understanding of the origin of the nonlinearities observed. Any changes in the modal gain can be measured in the near-field.

B. Time-Averaged Near-Field Investigations

The experimental setup for the near-field investigation is shown in Fig. 5. The emitted light is collected by a 0.65 NA microscope objective and passes through a Glan–Thompson polarizer to form a polarization-resolved image on the CCD array. A neutral density filter is used to avoid saturation of the CCD array. In order to minimize the optical feedback to the laser diode, the Glan–Thompson polarizer and the neutral density filters are set at a very slight angle to the beam. The beam is then focused down to a spot by a 25-cm focal length lens. The total magnification of the system was calibrated using a pinhole array and was found to be $\times$38.5. With this setup, we are able to observe the light distribution in the TE or the TM mode.

The near-field has been investigated in terms of its asymmetry. Fig. 6 shows an example the normalized intensity distribution as a function of the position along the plane of the active region recorded at a bias current of 17 mA and a temperature of 77 K. We can define x_0 as the position of the peak intensity, $\bar{x}$ as the position of the mean intensity given by

$$\bar{x} = \frac{\int xI(x)dx}{\int I(x)dx} \tag{1}$$

and σ the standard deviation by

$$\sigma = 2\sqrt{\frac{\int (x-\bar{x})^2 I(x)dx}{\int I(x)dx}}. \tag{2}$$

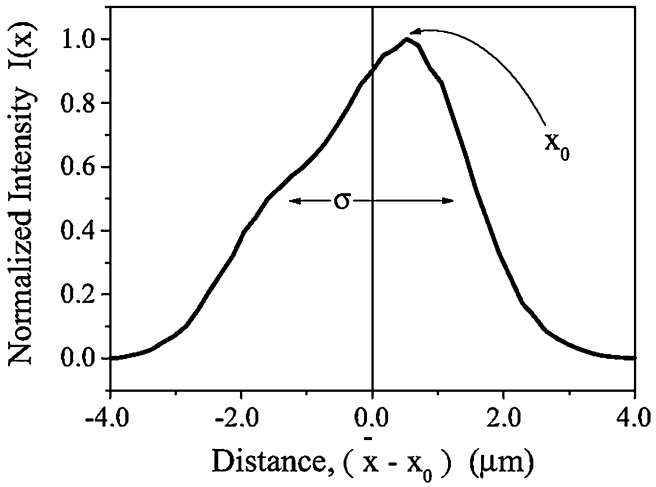

Fig. 6. Normalized intensity distribution of the TM-polarized emission, along the plane of the active region recorded at a bias current of 17 mA and a heatsink temperature of 77 K. Note the intensity distribution is centered on $\bar{x}$.

With the polarizer aligned in the plane of the TE-mode, the spatial intensity distribution of the stimulated emission is recorded. In contrast, when aligned in the plane of the TM-mode, it is the spontaneous emission that is recorded. These measurements have performed as a function of bias current and temperature. Fig. 7 shows the magnitude of the deviation between the position of the middle (or mean) of the near-field $\bar{x}$ and the position of the peak near-field power x_0 as a function of bias current, for four temperatures 77, 150, 230, and 310 K.

At 77 K, for non- and polarization resolved measurements of the magnitude $|\bar{x} - x_0|$ shows some similarity. Below threshold current, both magnitudes are identical. As the current increases, both magnitudes increase with bias. However, at 13 mA, the nonpolarization resolved magnitude decreases with bias, while the polarization resolved magnitude increases. At 17 mA, the polarization resolved magnitude reaches its maximum, and the nonpolarization resolved magnitude reaches its minimum. The distribution of the spontaneous emission is thus widely spread at this current. This bias corresponds to the bias at which the nonlinearity appears in the L–I curve shown in Fig. 4(b). Hence, the origin of this kink is due to a change in the modal gain. Beyond this bias, the polarization resolved-magnitude decreases with bias, the spontaneous emission is, therefore, more confined. At 20 mA and beyond, both magnitudes are of the same value. At temperatures above 77 K, for nonpolarization resolved, the magnitudes are almost constant with current and very close to zero, confirming the symmetry of near-field for all bias currents above the threshold current. In contrast, $|\bar{x} - x_0|$ for the TM-polarization-resolved SP near-field pattern is spread around zero until threshold and then increases monotonically with increasing bias current.

The key to understanding this observation is to remember that these near-field patterns are time-averaged, since the laser is SP at gigahertz frequencies. Typically, the duty cycle of these laser diodes is about 10% when it is exhibiting SP, as shown in Fig. 9. In the case of the nonpolarization observation, the average power of the stimulated emission signal is much larger than the spontaneous emission signal. Therefore, it must be

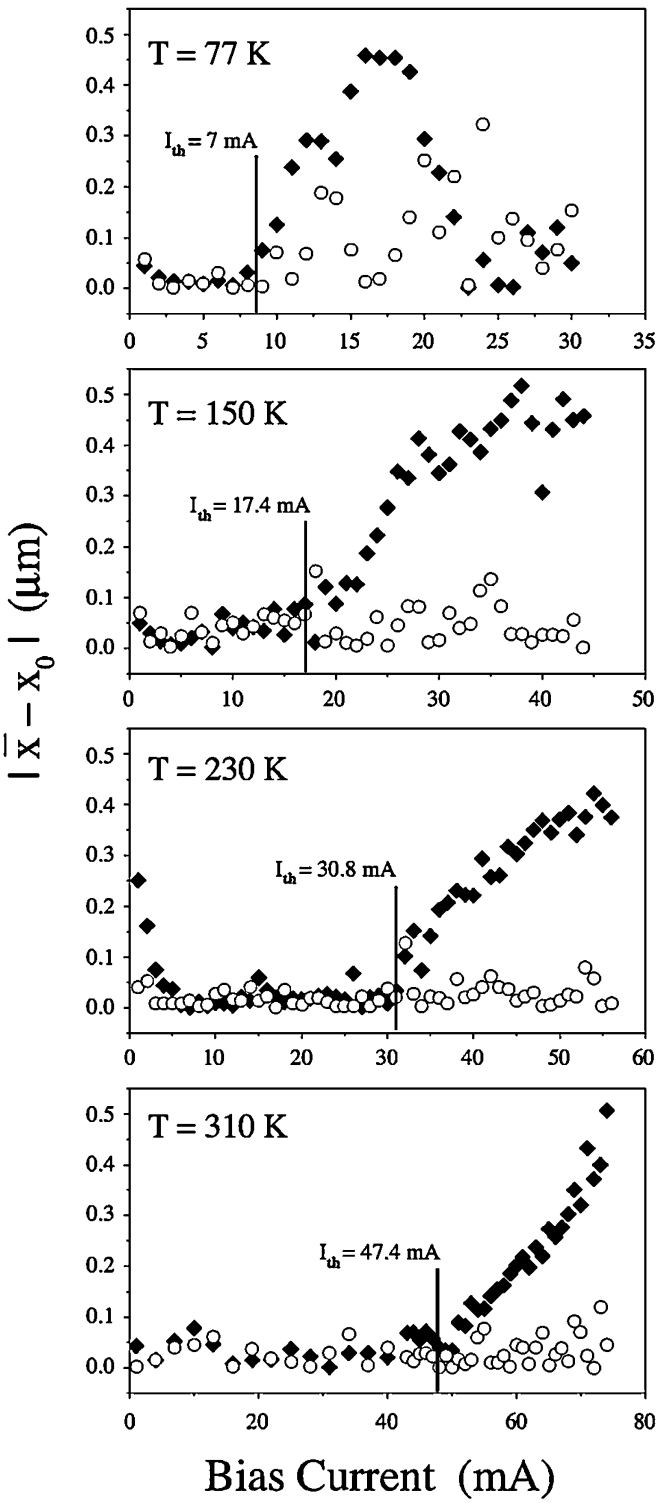

Fig. 7. Four graphs which show the variation of $|(\bar{x} - x_0)|$ for the SP near-field pattern with increasing bias current, for heatsink temperatures of 77, 150, 230, and 310 K. Nonpolarization-resolved emission data represented by open circles, and TM-polarization-resolved emission data by black diamond.

assumed that the near-field pattern is on average, symmetric during pulse emission. In the TM-polarization-resolved measurement, the stimulated emission signal is effectively blocked from reaching the detector. The light which is observed is then more representative of the time-averaged near-field pattern when the laser is in the other 90% of its duty cycle. Fig. 7

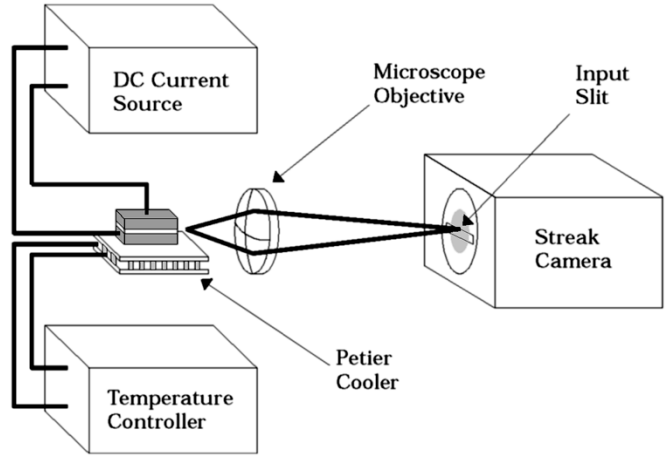

Fig. 8. Schematic of the experimental setup used to study the spatial and temporal evolution of the near-field.

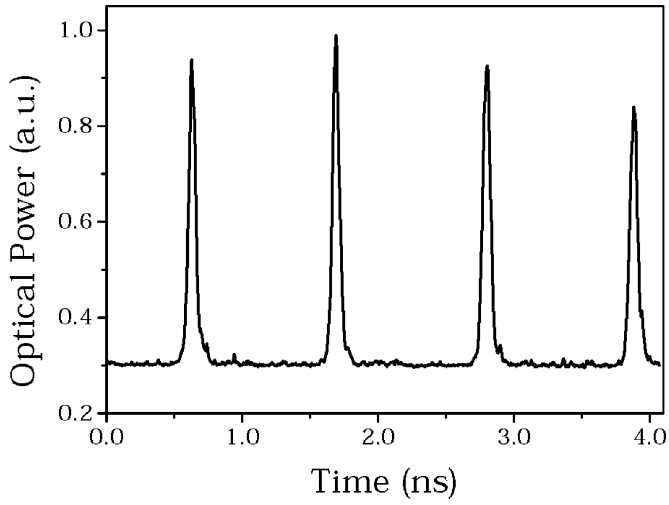

Fig. 9. Plot of the spatially integrated optical power emission as a function of time for a typical SHARP LT022MD laser diode. In this case, the bias current was 46 mA at a heatsink temperature of 310 K.

demonstrates discrepancy between the distribution of the lasing power and the spontaneous emission above threshold for the last three temperatures. The difference in the behavior of the nonpolarization-resolved and the polarization-resolved $|\bar{x} - x_0|$ is indirect evidence of a modification of the guiding in the laser cavity during the lasing process.

C. Real-Time Spatial Dynamics

Next, we have performed a real-time investigation of the near-field output. The relevant experimental setup for this measurement is depicted in Fig. 8. The emitted light is collected using a microscope objective, and focused on the input slit of a streak camera. No external modulation is applied to the laser diode in order to trigger the streak camera. In this way, we can be sure that there is no external influence that might otherwise affect to free-running SP dynamics, particularly in the manner described in [31].

First of all, Fig. 9 shows the spatially integrated optical power from the SP laser over a 4-ns time window. Four well-defined

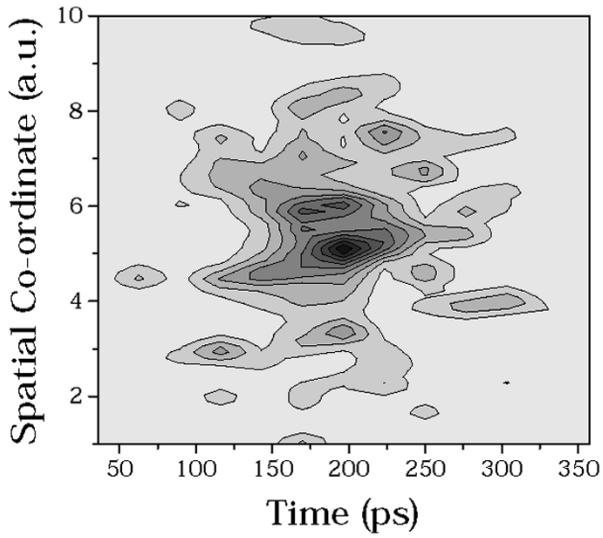

Fig. 10. Plot showing the evolution of the near-field along the plane of the active region for a typical SHARP LT022MD laser diode. In this case, the bias current was 45 mA at a heatsink temperature of 25 °C.

pulses can be seen. The time delay between each pulse is slightly longer than 1 ns, indicating a SP frequency just below 1 GHz.

Fig. 10 is an example of a contour plot showing the temporal evolution of the transverse intensity distribution of one of these pulses. Even though the signal to noise ratio is less than 10 dB, it is possible to discern the pulse evolution. The first signs of pulse emission begin at around 100 ps. As time progresses the pulse begins to broaden, reaching a maximum width between 175 and 225 ps. It is important to note, however, that the full-width at half-maximum (FWHM) of the intensity distribution actually narrows as time progresses because the optical power peaks sharply and is concentrated in a much smaller width. This is because the pulse is more tightly confined in the active region. By 250 ps, the apparent overall width of the pulse has narrowed again just before the lasing emission is extinguished. Much stronger evidence for this apparent behavior can be seen in Fig. 11. This figure shows the time evolution of the spatially integrated optical power (top) and of the standard deviation, σ, of the intensity distribution (bottom), calculated by integrating along the spatial coordinate of Fig. 11. In this case, σ gives a figure of merit which describes an effective width of the intensity distribution along the TE-mode. The standard deviation is a particularly useful figure of merit in this case since the very low signal to noise ratio does not otherwise allow a meaningful width (such as the FWHM) of the intensity distribution to be measured. In this bottom plot, the change in width of the intensity distribution is now very clear. At 100 ps, near the beginning of pulse emission, σ has a relatively large value around 0.9. As time progresses, the value of σ drops, reaching a minimum value of 0.55 between 175 and 225 ps. This is the point at which the pulse is most tightly confined and also corresponds (from the top plot) to the point at which the pulse reaches its peak power. By 250 ps, σ has returned to its original value of 0.9 just before the lasing emission is extinguished.

In Fig. 4(a), the slight increase in the TM-polarization resolved L–I curve above threshold current was attributed to gain suppression due to spectral, spatial-hole burning and/or carrier

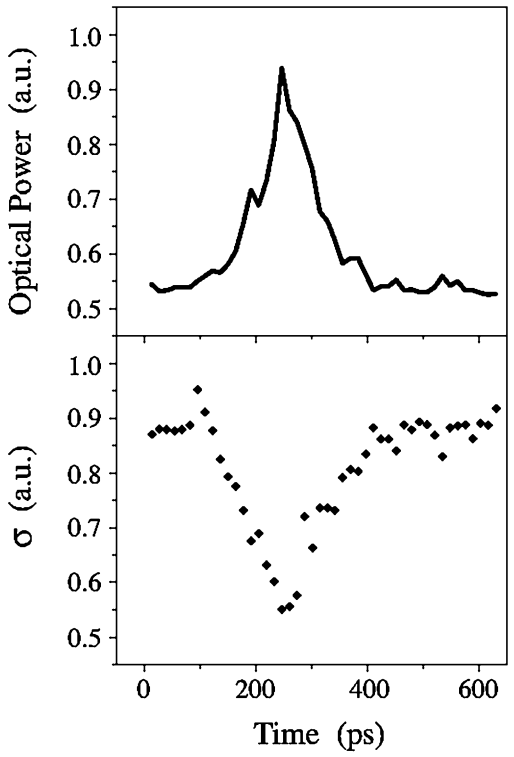

Fig. 11. (Top) Power output and (bottom) standard deviation σ as a function of time.

heating. In the same temperature condition, the real-time observation of the near-field shows that the optical mode becomes more strongly confined (almost 50%) as the pulse is generated in the optical cavity. The explanation for this behavior is as follows. During the pulse formation the carrier density increases in such a way that more carriers are found in the central electrically pumped gain section. This reduces the refractive index step between the central electrically pumped gain section and the surrounding unpumped regions. The net result is an antiguiding effect. Hence, the losses increase and more carriers are required. When the gain eventually equals the losses, the lasing condition is satisfied resulting in stimulated emission. As carriers begin to recombine the refractive index step becomes larger and the mode is more strongly confined. It is this interaction between antiguiding and self-focusing caused by spatial hole burning which is the true origin of the SP.

III. Discussion

The active region is pumped through a p-type electrical contact and the current is confined to the center by two n-type blocking layers on either side of the central region. These blocking layers create an effective refractive index profile in the lateral direction with a maximal value of refractive index in the center region to guide the optical mode. As the current is injected into the laser the large concentration of carriers toward the center tends to counterbalance this guiding by setting up a real antiguiding refractive index profile through the highly carrier density dependent complex refractive index. Due to this antiguiding effect the optical gain must increase to overcome the losses. Once the lasing condition is reached carriers recombine to create stimulated emitted photons. As the carrier density decreases the inherent effective index guiding of the blocking layers begins to dominate and less optical gain is required to overcome the losses in the cavity. Eventually the population inversion becomes depleted and the device can no longer sustain lasing. The carrier density must then recover before the conditions necessary for lasing are achieved again. The localized consumption of carriers, i.e., spatial-hole burning in the center, leads to a self-focusing of the lasing emission.

The SP phenomenon in this type of laser is generated by a modification of the waveguide, switching between self-focusing and antiguiding. This leads to a change of the losses. This spatial-hole burning manifests itself. In the steady state observation, it causes the increase of the spontaneous emission with bias current in Fig. 4(a). In the real time measurements, it produces antiguiding and self-focusing effects leading to a change of the cavity losses.

A key factor in the control of this proposed mechanism is the shape and magnitude of the step in the lateral refractive index profile. The shape and magnitude of this step will depend crucially on the transverse geometry of the laser structure, and on the refractive indexes of the surrounding material. Studies by Buus [32] have also shown that when the variation of the refractive index step is reduced from 4.5×10^{-3} to 1.5×10^{-3} the kink is more prominent. Furthermore, Stern [33] has shown that variation in refractive index due to free carrier absorption and gain variations is less at 77 K than at room temperature. Therefore, it is expected that as the temperature decreases from room temperature to low temperature the refractive index step will decrease and the kink become more prominent. In this regime of small refractive index step at low temperature, the self-focusing and antiguiding effects are no longer strong enough to generate the SP at the lower temperatures (as shown in Fig. 3). This explains the similarities of the lasing mode and spontaneous emission intensity distribution shown in Fig. 7. Thus, when the refractive index changes induced by the intensity are suppressed, the SP disappears. The spatial-hole burning is, therefore, the cause of the instability leading to the SP. In order to obtain robust SP in new material systems, the shape and magnitude of this step would have to be carefully chosen to optimize the guiding/antiguiding instability at lasing carrier densities predicted numerically in multiquantum-well lasers [34]. Similar behavior in broad stripe laser diodes have been investigated both experimentally by Paoli [35] and van der Ziel [36], and theoretically by Buus [32].

IV. Conclusions

By using a combination of polarization-resolved time-averaged near-field measurements and streak camera measurements, we have shown that waveguide instabilities are synonymous with CD lasers. At low temperatures when the lasing emission is continuous-wave, nonlinearity in the L–I curves are observed and can be attributed to nonuniformities and asymmetries in the waveguide which lead to preferential guiding of the optical mode off center [32]. As the temperature is increased, higher carrier densities are required to reach the same value of optical

gain. The increased antiguiding due to this larger carrier density leads to an instability in the waveguide which results in SP. We have observed this antiguiding effect in real-time, thus confirming our hypothesis that SP in these devices arises from the interplay between inherent effective index guiding of the cladding and blocking layers, and the antiguiding which results from the presence of carriers in the active region.

Consequently from a simulation point of view, the rate-equation model is still a reliable tool to predict the behavior of CD lasers, but it should include the spatial-hole burning. This will appear as a modification of the confinement factor as the function of the photon density in order to take into the waveguide fluctuation. Of course, to obtain a complete representation of the SP dynamics it would be necessary to move to a full two–dimensional model such as [34].

These results have important consequences for the future design of SP lasers. In order to obtain robust SP in other material systems, considerable care must be taken when choosing the thickness and doping of the various layers, which in turn is necessary to obtain the optimum effective index profile with pumping, leading to the waveguiding instability that causes SP.

ACKNOWLEDGMENT

The authors would like to thank all of the reviewers for their insightful and helpful comments. They believe that the implementation of the reviewer's suggestions and corrections has greatly strengthened this paper.

REFERENCES

[1] N. G. Basov, "Dynamics of injection lasers," *IEEE J. Quantum Electron.*, vol. QE-4, no. 11, pp. 855–867, Nov. 1968.

[2] E. S. Yang, P. G. McMullin, A. W. Smith, J. Blum, and J. Shih, "Degradation induced microwave oscillations in double-heterostructure lasers," *Appl. Phys. Lett.*, vol. 2, pp. 324–326, 1974.

[3] J. P. van der Zeil, J. L. Merz, and T. L. Paoli, "Study of intensity pulsations in proton-bombarded stripe-geometry double-heterostructure AlGaAs lasers," *J. Appl. Phys.*, vol. 50, no. 7, pp. 4620–4637, 1979.

[4] M. Ueno and R. Lang, "Conditions for self-sustained pulsation and bistability in semiconductor lasers," *J. Appl. Phys.*, vol. 58, pp. 1689–1692, 1985.

[5] M. Yamada, "A theoretical analysis of self-sustained pulsation phenomena in narrow stripe semiconductor lasers," *IEEE J. Quantum. Electron.*, vol. 29, no. 5, pp. 1330–1336, May 1993.

[6] A. Scire, J. Mulet, C. R. Mirasso, and M. San Miguel, "Polarization properties of self-pulsating VCSELs," in *Proc. IEEE/LEOS Summer Topics*, 2002, pp. TuP6-51–TuP6-52.

[7] C. R. Mirasso, G. H. M. Van Tartwijk, E. Hernandez-Garcia, D. Lenstra, S. Lynch, P. Landais, P. Phelan, J. O'Gorman, M. San Miguel, and W. Elsäßer, "Self-pulsating semiconductor lasers: theory and experiment," *IEEE J. Quantum. Electron.*, vol. 35, no. 5, pp. 764–770, May 1999.

[8] J. L. A. Dubbeldam and B. Krauskopf, "Self-pulsations of lasers with saturable absorber: dynamics and bifurcations," *Opt. Commun.*, vol. 159, pp. 325–338, 1999.

[9] B. Sartorius, M. Möhrle, S. Reichenbacher, H. Preier, H.-J. Wünsche, and U. Bandelow, "Dispersive self-Q-switching in self-pulsating DFB lasers," *IEEE J. Quantum. Electron.*, vol. 33, no. 2, pp. 211–218, Feb. 1997.

[10] U. Bandelow, M. Radziunas, J. Sieber, and M. Wolfrum, "Impact of gain dispersion on the spatio-temporal dynamics of multisection lasers," *IEEE J. Quantum. Electron.*, vol. 37, no. 2, pp. 183–188, Feb. 2001.

[11] G.-H. Duan and P. Landais, "Self-pulsation in multielectrode distributed feedback laser," *IEEE Photon. Technol. Lett.*, vol. 7, no. 3, pp. 278–280, Mar. 1995.

[12] A. J. Lowery, "Dynamics of SHB-induced mode instabilities in uniform DFB semiconductor lasers," *Electron. Lett.*, vol. 29, pp. 1852–1854, 1993.

[13] D. D. Marcenac and J. E. Carroll, "Distinction between multimoded and single-moded self-pulsations in DFB lasers," *Electron. Lett.*, vol. 30, pp. 1137–1138, 1994.

[14] R. Schatz, "Longitudinal spatial instability in symmetric semiconductor lasers due to spatial hole burning," *IEEE J. Quantum Electron.*, vol. 28, no. 9, pp. 1443–1449, Sep. 1992.

[15] U. Bandelow, H.-J. Wünsche, and H. Wenzel, "Theory of self-pulsations in two-section DFB lasers," *IEEE Photon. Technol. Lett.*, vol. 5, no. 10, pp. 1176–1179, Oct. 1993.

[16] J. Renaudier, G.-H. Duan, J.-G. Provost, H. Debregeas-Sillard, and P. Gallion, "Phase correlation between longitudinal modes in semiconductor self-pulsating DBR lasers," *IEEE Photon. Technol. Lett.*, vol. 17, no. 4, pp. 741–743, Apr. 2005.

[17] P. Landais, J. Renaudier, and G. H. Duan, "Analysis of self-pulsation in distributed Bragg reflector laser based on four-wave mixing," *Soc. Photo-Opt. Instrum. Eng., Phys. Simulation Optoelectron. Dev. XII*, vol. 5349, pp. 263–270, Jan. 2004.

[18] P. Bardella and I. Montrosset, "Analysis of self-pulsating three-section DBR lasers," *IEEE J. Sel. Topics Quantum Electron.*, vol. 11, no. 2, pp. 361–366, Mar./Apr. 2005.

[19] M. Jinno and T. Matsumoto, "Nonlinear operations of 1.55 μm wavelength multielectrode distributed-feedback laser diodes and their applications for optical signal processing," *J. Lightw. Technol.*, vol. 29, no. 4, pp. 448–457, Apr. 1992.

[20] K. E. Chlouverakis and M. J. Adams, "Two-section semiconductor lasers subject to optical injection," *IEEE J. Sel. Topics Quantum Electron.*, vol. 10, pp. 982–990, 2004.

[21] I. Pierce, H. D. Summers, P. Rees, and D. R. Jones, "Multi-mode self-pulsation in laser diodes with epitaxially integrated saturable absorbers: mode competition and carrier dynamics," *Proc. IEE Optoelectron.*, vol. 150, pp. 159–162, 2003.

[22] S. E. M. Dudley, J. M. Guzman, T. Quinlan, and S. D. Walker, "Direct off-air transmission and tunable bandpass filtering using self-pulsating lasers and substrate antannae," *J. Lightw. Technol.*, vol. 23, no. 2, pp. 809–817, Feb. 2005.

[23] C. Harder, K. Y. Lau, and A. Yariv, "Bistability and pulsations in semiconductor lasers with inhomogeneous current injection," *IEEE J. Quantum Electron.*, vol. QE-29, no. 9, pp. 1351–1361, Sep. 1982.

[24] S. Matsui, H. Takiguchi, H. Hayashi, S. Yamamoto, and T. Hijikata, "Suppression of feedback-induced noise in short-cavity V channeled substrate inner stripe lasers with self-oscillation," *Appl. Phys. Lett.*, vol. 43, pp. 219–221, 1983.

[25] A. Kaszubowska, L. P. Barry, and P. Anandarajah, "Effects of intermodulation distortion on the performance of a hybrid radio/fiber system employing a self-pulsating laser diode transmitter," *IEEE Photon. Technol. Lett.*, vol. 15, no. 6, pp. 852–854, Jun. 2003.

[26] G. P. Agrawal and N. K. Dutta, *Long-Wavelength Semiconductor Lasers*. New York: Van Nostrand Reinhold, 1986.

[27] L. A. Coldren and S. W. Corzine, *Diode Lasers and Photonic Integrated Circuits*. New York: Wiley, 1995.

[28] R. Nagarajan, M. Ishikawa, T. Fukushima, R. S. Geels, and J. Bowers, "High speed quantum-well lasers and carrier transport effects," *IEEE J. Quantum Electron.*, vol. 28, no. 10, pp. 1990–2008, Oct. 1992.

[29] S. Lynch, P. McEvoy, P. Landais, J. O'Gorman, J. Hegarty, and W. Elsäßer, "Temperature dependence of self-pulsation in narrow stripe, gain guided, compact disc laser diodes," in *Laser Diodes and Applications III*, P. Galarneau, Ed. Bellingham, WA: SPIE, Jul. 1998, vol. 3415.

[30] S. A. Lynch, P. McEvoy, P. Landais, J. O'Gorman, P. Rees, W. Elsäßer, and P. Landais, "Temperature dependence of self-pulsation in compact disc lasers," *Proc. IEE Optoelectron.*, vol. 151, pp. 496–501, 2004.

[31] A. Egan, M. Harley-Stead, P. Rees, S. Lynch, J. O'Gorman, and J. Hegarty, "An experimental and theoretical analysis of jitter in self-pulsating lasers synchronised to periodic electrical signals," *IEEE Photon. Technol. Lett.*, vol. 8, no. 6, pp. 758–760, Jun. 1996.

[32] J. Buus, "Models of the static and dynamic behavior of stripe geometry lasers," *IEEE J. Quantum Electron.*, vol. QE-19, no. 6, pp. 953–960, Jun. 1983.

[33] F. Stern, "Calculated spectral dependence of gain in excited GaAs," *J. Appl. Phys.*, vol. 47, no. 8, pp. 5382–5386, Dec. 1976.

[34] T. Takayama, O. Imafuji, M. Yuri, H. Naito, M. Kume, A. Yoshikawa, and K. Itoh, "800 mW peak-power self-sustained pulsation GaAlAs laser diodes," *IEEE J. Sel. Topics Quantum Electron.*, vol. 1, no. 2, pp. 562–568, Jun. 1995.

[35] T. L. Paoli, "Nonlinearities in the emission characteristics of stripe geometry (AlGa)As double-heterostructure junction lasers," *IEEE J. Quantum Electron.*, vol. QE-12, no. 12, pp. 770–776, Dec. 1976.

[36] J. P. van der Ziel, "Self-focusing effects in pulsating AlGaAs double-heterostructure lasers," *IEEE J. Quantum Electron*, vol. QE-17, no. 1, pp. 60–68, Jan. 1981.

Pascal Landais (M'02) received the Ph.D. degree in applied physics from the Ecole Nationale Supérieure des Télécommunications, Paris, France, in 1995, where he studied bistable and self-pulsating semiconductor lasers as all-optical functional components in fiber telecommunication systems.

In 1996, he joined the Physics Department, Trinity College, Dublin, Ireland, where he developed low-coherence semiconductor lasers for data storage and stabilized Fabry–Perot lasers. Between 1997 and 1999, he was involved in research activities on microcavity light-emitting diodes under the European project SMILED. Between 1999 and 2000, he was a Development Manager in CeramOptec Ltd., Ireland. Since January 2001, he has been a Lecturer in the School of Electronic Engineering, Dublin City University, Dublin, Ireland, where he has since developed, and currently directs research, on components for optical communication systems and terahertz generation. His group is part of the Research Institute for Networks and Communications Engineering, known as RINCE.

Dr. Landais is a TMR Marie Curie Fellow.

Stephen A. Lynch (SM'05) was born in Drogheda, County Louth, Ireland, on April 11, 973. He received the B.Sc. degree (first class hons.) in experimental physics from University College Dublin, Dublin, Ireland, in 1995. He received the Ph.D. degree from Trinity College, Dublin, in 1999 for work on pulse formation and dynamics in self-pulsating semiconductor laser diodes

From October 1996 to January 1997, he worked at the Ecole Nationale Superieure des Telecommunications, Paris, France, on high-frequency self-pulsation in distributed feedback lasers for telecommunications applications. From October 1999 to February 2000, he worked on Amber-Green Emission Targeted at High Temperature Applications (AGETHA), IST-1999-10 292, an European Union (EU) project supported under the Fifth Framework. He joined the Semiconductor Physics Group, Cavendish Laboratory, Cambridge, U.K., in February 2000. He is joint Coordinator (with Dr. D. J. Paul) of Silicon Heterostructure Intersubband Emitters (SHINE), IST-2001-38 035, an EU project supported under the Fifth Framework. His current research interests include terahertz source and detector development, quantum-cascade lasers, and secure telecommunications using chaotic encryption in pulsed laser diodes.

Dr. Lynch was elected a Research Fellow of St Edmund's College, Cambridge, in 2002 and also holds an Isaac Newton Trust teaching fellowship.

James O'Gorman received the Ph.D. degree in laser physics from Trinity College, Dublin, Ireland, in 1989.

He is the Founder and CEO of Eblana Photonics with J. Hegarty. He was Professor of laser physics and Provost of Trinity College Dublin. Subsequently, he joined Bell Laboratories, the research and development arm of AT&T (now Lucent Technologies) where he carried out research on high-speed laser diode design and high-speed data communications applications using laser diodes and laser diode arrays for access and enterprise applications. Prior to Founding Eblana, he was General Manager in Trinity College of Optronics Ireland—the Irish National program for commercialization of Optics in Ireland.

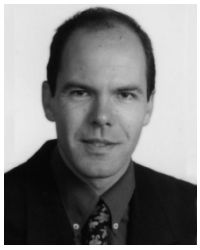

Ingo Fischer was born in Marburg, Germany, in 1966. He received the diploma and Ph.D. degrees in physics from the Philipps University, Marburg, Germany, in 1992 and 1995, respectively.

In 1995, he joined the Institute of Applied Physics, Darmstadt University of Technology, Darmstadt, Germany, where his research activities were centered around spatial, spectral, and dynamical emission properties of semiconductor lasers. His studies concentrate on nonlinear dynamics, synchronization of coupled lasers, VCSEL emission, high-power laser emission, femtosecond spectroscopy and THz generation. He has had research stays with Air Force Research Laboratories, Albuquerque, NM, in 1999, with ATR, Kyoto, Japan, in 1999 and 2000, and with UIB, Palma de Mallorca, Spain, in 2004. Since 2005, Dr. Fischer has been with the Vrije Universiteit Brussels, Brussels, Belgium.

Dr. Fischer received the Research Prize of the Adolf-Messer Foundation in 2000 and the first Hassian Cooperation Prize of the Technology Transfer Network in 2004.

Wolfgang Elsäßer (M'94–SM'97) was born in Pforzheim, Germany, in 1954. He received the diploma degree in physics from the Technical University of Karlsruhe, Karlsruhe, Germany, in 1980, the Ph.D. degree in physics from the University Stuttgart, Stuttgart, Germany, in 1984, and the Habilitation degree in experimental physics from the Philipps-University Marburg, Marburg, Germany, in 1991.

From 1981 to 1985, he was with the Max-Planck-Institute for Solid State Research, Stuttgart, Germany. From 1985 to 1995, he was with Philipps-University Marburg. Since 1995, he has been a Full Professor in the Institute for Applied Physics, Darmstadt University of Technology, Darmstadt, Germany. He was on sabbatical leave in 1992 with the Ecole Nationale Superieure des Telecommunications, Paris, France. His research stays have included Trinity College, Dublin, Ireland, in 1990, 1996, 1999, and 2000.

Dr. Elsäßer is a Member of the German Physical Society (DPG). He was awarded the Otto-Hahn-Medal (1985), the Werner-von-Siemens-Medal (1985), the Rudolf-Kaiser Prize (1991), and the Institute of Electrical Engineers (IEE) J. J. Thomson Premium (1995).